Active acetyl-CoA synthase from *Clostridium thermoaceticum* obtained by cloning and heterologous expression of *acsAB* in *Escherichia coli*

Huay-Keng Loke*, George N. Bennett†, and Paul A. Lindahl*‡§

*Departments of Chemistry and ‡Biochemistry and Biophysics, Texas A&M University, College Station, TX 77843; and †Department of Biochemistry and Cell Biology, Rice University, Houston, TX 77005

Communicated by Helmut Beinert, University of Wisconsin, Madison, WI, August 23, 2000 (received for review September 16, 1999)

Acetyl-CoA synthase from *Clostridium thermoaceticum* (ACS_{Ct}) is an $\alpha_2\beta_2$ tetramer containing two novel Ni-X-Fe_4S_4 active sites (the A and C clusters) and a standard Fe_4S_4 cluster (the B cluster). The *acsA* and *acsB* genes encoding the enzyme were cloned into *Escherichia coli* strain JM109 and overexpressed at 37°C under anaerobic conditions with Ni supplementation. The isolated recombinant His-tagged protein (AcsAB) exhibited characteristics essentially indistinguishable from those of ACS_{Ct}, from which Ni had been removed from the A cluster. AcsAB migrated through nondenaturing electrophoretic gels as a single band and contained a 1:1 molar ratio of subunits and 1.0–1.6 Ni/$\alpha\beta$ and 14–22 Fe/$\alpha\beta$. AcsAB exhibited 100–250 units/mg CO oxidation activity but no CO/acetyl–CoA exchange activity. Electronic absorption spectra of thionin-oxidized and CO-reduced AcsAB were similar to those of ACS_{Ct}, with features typical of redox-active Fe_4S_4 clusters. Partially oxidized and CO-reduced AcsAB exhibited EPR signals with *g* values and low spin intensities indistinguishable from those of the B_{red} state of the B cluster and the C_{red1} and C_{red2} states of the C cluster of ACS_{Ct}. Upon overnight exposure to $NiCl_2$, the resulting recombinant enzyme (ACS_{Ec}) developed 0.06–0.25 units/mg exchange activity. The highest of these values is typical of fully active ACS_{Ct}. When reduced with CO, ACS_{Ec} exhibited an EPR signal indistinguishable from the NiFeC signal of Ni-replete ACS_{Ct}. Variability of activities and signal intensities were observed among different preparations. Issues involving the assembly of these metal centers in *E. coli* are discussed.

Certain archaea and bacteria grow chemoautotrophically using the Wood/Ljungdahl pathway (1). The central enzyme of this pathway is acetyl-CoA synthase (ACS), also called carbon monoxide dehydrogenase (CODH). The enzyme from *Clostridium thermoaceticum* (ACS_{Ct}) catalyzes two reactions, including the reversible reduction of CO_2 to CO, and the synthesis of acetyl-CoA from CO, CoA, and a methyl group bound to a corrinoid-iron-sulfur protein (2). This corrinoid protein is methylated by methyltetrahydrofolate in a reaction catalyzed by a methyltransferase.

ACS_{Ct} is an $\alpha_2\beta_2$ tetramer containing three types of metal-sulfur clusters called A, B, and C (2, 3). The B and C clusters are located in the β subunit, whereas the A cluster is located in α. The B cluster is a standard $[Fe_4S_4]^{2+/1+}$ cluster involved in electron transfer (4), and it exhibits an EPR signal with $g_{av} = 1.94$ when reduced to the B_{red} state (5). The C cluster is the active site for CO_2/CO redox catalysis (6–9) and likely consists of an Ni complex weakly coupled through an unidentified bridge to an Fe_4S_4 cluster (10, 11). The one- and three-electron reduced C_{red1} and C_{red2} states exhibit EPR signals with $g_{av} = 1.82$ and 1.86, respectively. The A cluster is the active site for acetyl-CoA synthesis and is also composed of an Ni center bridged to an Fe_4S_4 cluster (12–15). The Ni ion of the A cluster is labile and can be removed easily by incubating ACS_{Ct} in the chelator 1,10-phenanthroline. The Ni ion is readily reinserted by incubating phenanthroline-treated enzyme with $NiCl_2$ (13–15). When the A cluster is reduced by one electron and bound with CO, it yields a state (A_{red}-CO) that exhibits the so-called NiFeC EPR signal ($g = 2.08, 2.07, 2.03$). For unknown reasons, only a fraction of the A, B, and C clusters are redox and catalytically active (16). This heterogeneity is reflected in the low spin intensities of the NiFeC, $g_{av} = 1.94$, 1.82, and 1.86 signals (≈0.2, 0.6, 0.3, and 0.3 spins/$\alpha\beta$, respectively).

In *C. thermoaceticum*, the enzymes involved in the Wood/Ljungdahl pathway are encoded by the *acs* genes (17–19). Genes *acsA* and *acsB* encode the β and α subunits of ACS_{Ct}, respectively. Genes *acsC* and *acsD* encode the corrinoid-iron-sulfur protein subunits, and *acsE* encodes methyltransferase. The *acs* genes contain promoter-like sequences and translational signals that are recognized by *Escherichia coli*. Roberts *et al.* have cloned and expressed these genes in *E. coli* and found that only AcsE was catalytically active (17, 19). AcsCD was inactive but could be activated by incubation with cobalamin, iron, and sulfide ions (20). AcsAB was inactive, but a method of activation has not been reported. Roberts *et al.* reported that the recombinant α and β subunits migrated independently on nondenaturing electrophoretic gels, indicating the absence of the native tetrameric structure (17). They suggested that AcsAB was inactive because the bacteria were grown aerobically without metal ion supplementation. Morton *et al.* (19) later suggested that recombinant subunits might lack competent NiFeS centers. Genes encoding ACS homologs in methanogenic archaea have been sequenced, cloned, and/or overexpressed in *E. coli* (21–28), but to our knowledge no active recombinant enzyme from a methanogen has been reported.

The purple nonsulfur photosynthetic *Rhodospirillum rubrum* contains a monomeric carbon monoxide dehydrogenase homologous to the β subunit of ACS_{Ct} (29). $CODH_{Rr}$ exclusively catalyzes the reversible oxidation of CO to CO_2 (30) and contains only the B and C clusters. The *cooS* gene encoding this enzyme has been cloned and sequenced (31). Using conjugative mating followed by homologous recombination, the gene was introduced into a strain of *R. rubrum* lacking functional $CODH_{Rr}$. This elegant method afforded functional enzyme and

Abbreviations: ACS_{Ct}, acetyl-CoA synthase from *C. thermoaceticum*, also called carbon monoxide dehydrogenase or $CODH_{Ct}$; AcsAB, isolated His-tagged protein produced by expressing *C. thermoaceticum acsA* and *acsB* genes in *E. coli*; ACS_{Ec}, AcsAB after activating with $NiCl_2$; $CODH_{Rr}$, carbon monoxide dehydrogenase from *R. rubrum*; Ni-NTA, Ni-nitrilotriacetic acid.

§To whom reprint requests should be addressed.

The publication costs of this article were defrayed in part by page charge payment. This article must therefore be hereby marked "*advertisement*" in accordance with 18 U.S.C. §1734 solely to indicate this fact.

Article published online before print: *Proc. Natl. Acad. Sci. USA*, 10.1073/pnas.220404397. Article and publication date are at www.pnas.org/cgi/doi/10.1073/pnas.220404397

allowed the construction and study of numerous functional site-directed mutants (32, 33). It has also allowed consideration of issues involving the assembly of the metal-sulfur clusters. Roberts and coworkers have identified three genes (*cooCTJ*), deletions in which result in Ni-deficient $CODH_{Rr}$ (31). This suggests that CooC, CooT, and CooJ play roles in inserting Ni into CooS during maturation. CooC possesses a nucleotide-binding "P-loop" region and is homologous to GTPases required to insert Ni into urease and NiFe hydrogenases (34–37).

Given the tremendous utility of recombinant metalloenzyme systems, we wanted to generate active enzyme by overexpressing cloned *acsAB*. However, because of the reported inability of *E. coli* to serve as a host for this, our strategy was to clone and manipulate *acsA* and *acsB* in *E. coli* and then introduce them into a host containing accessory proteins required for ACS metal cluster assembly. In this paper, we describe the surprising result that the purified recombinant AcsAB from *E. coli* is a tetramer that contains assembled B and C clusters and exhibits CO oxidation activity levels typical of native ACS_{Ct}. Furthermore, the recombinant protein can be activated by treatment with $NiCl_2$ to afford CO/acetyl-CoA exchange activity and the NiFeC EPR signal, indicative of assembled A cluster. Thus, the activated recombinant protein is essentially indistinguishable from native ACS_{Ct}. Implications of these results for probing the mechanism of cluster assembly and the origin of heterogeneity are discussed.

Materials and Methods

Materials. Restriction enzymes, T4 DNA ligase, alkaline phosphatase, isopropylthio-β-D-galactoside and anti-rabbit IgG (Fc) AP conjugate were from Promega. *Taq* polymerase was from Perkin–Elmer. Ni-nitrilotriacetic acid (Ni-NTA) agarose, *E. coli* strain M15(pREP4), QiaPrep spin miniprep kit, QIAquick PCR purification kit, and vector pQE-60 were purchased from Qiagen. This vector was used to install a His-tag at the C terminus of the α subunit of cloned *acsAB*. Anti-ACS_{Ct} rabbit serum was prepared by Alpha Diagnostics (San Antonio, TX).

Cloning of *acsAB*. *C. thermoaceticum* cells were grown as described (38) under CO_2/H_2 in a Coy Laboratory Instruments chamber. Genomic DNA was isolated using the DNA isolation kit from Puregene. PCR primers 5′-GGCGAGATCTGAATTCATCCTCAACCAC-3′ and 5′-GGCGAGATCTCATAATGGGATCCATGGT-3′, designed to hybridize to the ends of *acsA* and *acsB*, were synthesized by Genosys (The Woodlands, TX). Genes *acsAB* were amplified from genomic DNA using these primers, a Stratagene Gradient 96 Robocycler, and a PCR optimizer kit (Invitrogen). The resulting 4.5-kilobase PCR product was purified with the QIAquick PCR purification kit and digested with *Bgl*II. Vector pQE-60 was digested with *Bgl*II and incubated with alkaline phosphatase to prevent self-ligation. The digested vector and PCR product were ligated and transformed into M15(pREP4) competent cells. Plasmid pT316 was isolated from kanamycin- and ampicillin-resistant colonies.

Double-strand sequencing by the Gene Technologies Laboratory (Department of Biology, Texas A&M University) revealed that pT316 contained *acsAB*, albeit with three mutations relative to that reported by Morton *et al.* (19). One mutation was silent, one yielded Ser instead of Pro at position 259 in AcsA, and the third yielded Asp instead of Glu at position 527 of AcsB. A second cloning (from genomic DNA) and sequencing of the two affected regions indicated Pro-259 in AcsA and Asp-527 in AcsB. This suggests that native *acsA* and *acsB* encode Pro-259 and Asp-527, respectively. The QuikChange site-directed mutagenesis kit (Stratagene) was subsequently used to change Ser-259 to Pro-259. The resulting plasmid, pTM02, was subsequently transformed and expressed in *E. coli* strain JM109 [*e14-(McrA-) recA1 endA1 gyrA96 thi-1 hsdR17*(r_K^- m_K^+) *supE44 relA1* Δ*(lac-proAB) F′ traD36 proAB lacI*^{q}*Z*Δ*M15*] (Stratagene).

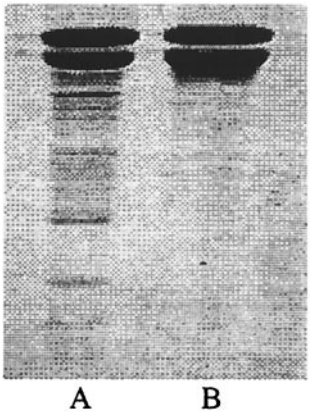

Fig. 1. SDS/PAGE gel (12%) of ACS_{Ct} (*A*) and AcsAB (*B*).

Expression of AcsAB. *E. coli* JM109 (pTM02) cells were grown in 25 liters of Begg's medium (1% tryptone/0.5% yeast extract/0.4% glucose/100 mM potassium phosphate, pH 6.5/15 mM sodium formate/1 μM sodium molybdate/1 μM sodium selenite/5 μM $NiCl_2$) (39) under stirred (100 rpm) anaerobic (N_2) conditions using a custom-made (Chemglass, Inc.) water-jacketed all-glass Bioreactor maintained at 37°C with a refrigerated recirculator (Polysciences). When the optical density of cells reached 0.65–0.75 at 600 nm (1-cm path length), isopropylthio-β-D-galactoside and $NiCl_2$ were added to final concentrations of 0.1 and 0.5 mM, respectively. Cells were harvested anaerobically and frozen in liquid N_2. The presence of AcsAB, and thus the expression of *acsAB*, was indicated by Western blotting (40).

Purification of AcsAB. Using standard anaerobic methods (38), 70 g of frozen cells, 70 mg of lysozyme, and a trace of DNase were suspended in 350 ml of buffer A (50 mM NaP_i, pH 8.0/0.3 M NaCl/10 mM β-mercaptoethanol). After 1 h, the suspension was sonicated (Branson Sonifier 450) at room temperature for 5 min using 1-s pulses (duty cycle constant 60% and output control 7), and then centrifuged at 23,500 × *g* with a GSA rotor (Sorvall) for 1.5 h. The supernatant was loaded onto an Ni-NTA agarose column (1.6 × 12 cm) equilibrated in buffer A. The column was washed with 100 ml of 10 mM imidazole in buffer A and then eluted with 100 mM imidazole in buffer A. The brown-colored eluent was diluted 4× with buffer B (50 mM Tris-Cl, pH 8.0/10 mM DTT/2 mM sodium dithionite) and loaded on a DEAE column (2.6 × 15 cm) equilibrated in buffer B. The column was washed with 150 ml of 0.2 M NaCl in buffer B followed by 300 ml of a 0.2–0.4 M gradient of NaCl in buffer B. Fractions exhibiting CO oxidation activity were combined, concentrated, and frozen in liquid N_2.

One batch of AcsAB was isolated as described (38) without the use of the Ni-NTA agarose column and further purified by FPLC, as described (41) using a POROS 50D column (PerSeptive Biosystems, Framingham, MA), equilibrated in buffer C (50 mM Tris, pH 8.0). After loading, the column was washed with 125 ml of 0.1 M NaCl in buffer C and eluted with 125 ml of a 0.1–0.4 M gradient of NaCl in buffer C.

Characterization and Activation of AcsAB. Sample purity was quantified by scanning Coomassie blue-stained SDS/PAGE gels with an AlphaImager 2000 (Alpha Innotech, San Leandro, CA) densitometer. Native gel electrophoresis was performed anaer-

Table 1. Characteristics of purified AcsAB before and after Ni activation

Batch	1	2	3
Mass of cell paste (g)	70	65	80
Ni content before activation (Ni/$\alpha\beta$)	1.5	1.6	1.0
Fe content before activation (Fe/$\alpha\beta$)	16	22	14
CO oxidation activity before/after activation (units/mg)	160/140	200(220)/250	100(90)/100
CO exchange activity before/after activation (units/mg)	0/0.06	0/0.15	0/0.25
NiFeC Signal intensity before/after activation (spin/$\alpha\beta$)	0/0.15	0/0.38	0/0.15
g_{av} = 1.94 Signal intensity before/after activation (spin/$\alpha\beta$)	1.12/0.75	0.95(0.55)/0.93	0.83(0.66)/0.82
g_{av} = 1.82 Signal intensity before activation (spin/$\alpha\beta$)	0.29	0.31	0.25
g_{av} = 1.86 Signal intensity before/after activation (spin/$\alpha\beta$)	0.21/0.24	0.13/0.18	0.08/0.09

Batch 1 was activated with Ni under 1 atm Ar, while batches 2 and 3 were activated under 1 atm CO. Values in parentheses for batches 2 and 3 are from samples incubated overnight in the absence of reductants and under 1 atm Ar.

obically as described (42). CO oxidation and CO/acetyl-CoA exchange activities were performed as described (38, 43). The Ni and Fe contents of purified AcsAB were determined using atomic absorption spectrometry (12). EPR spectra of AcsAB were determined using a Bruker ESP300 spectrometer and an Oxford Instruments ER910A cryostat. Signals were quantified as described (44) using a 1.00 mM CuEDTA standard. UV-visible absorption spectra were determined using a Beckman DU 640B spectrophotometer. Samples were freed from reductant by passage through a column of Sephadex G-25 (1 × 17 cm) equilibrated in buffer D (100 mM Mops, pH 7.5). A sample was transferred to a quartz cuvette that was subsequently sealed with a septum and removed from the glove box. Thionin solution was added until a weak band at 600 nm appeared because of oxidized thionin, ensuring a fully oxidized sample. Another sample was reduced by exposure to 1 atm (1 atm = 101.3 kPa) CO. Protein concentrations were determined as described (45) using BSA as a standard. The A cluster of reductant-free AcsAB (≈3–8 mg/ml^{-1}) in buffer D was activated by incubation with 200 μM (final concentration) $NiCl_2$ overnight under an Ar or CO atmosphere at room temperature.

Results

Genes *acsA* and *acsB* from *C. thermoaceticum* were cloned and overexpressed in *E. coli*. The recombinant protein AcsAB contained a His-tag, which allowed rapid purification. Samples were >95% pure according to densitometric analysis of SDS/PAGE gels. AcsAB consisted of two subunits that migrated, in SDS/PAGE gels, at the same rates as the α and β subunits of ACS_{Ct} (Fig. 1). Based on relative staining densities, the α and β recombinant subunits were present in a 1:1 molar ratio. Moreover, AcsAB had the same mobility as ACS_{Ct} on a nondenaturing electrophoresis gel (data not shown). These results suggest that AcsAB possesses the same $\alpha_2\beta_2$ tetrameric structure as ACS_{Ct}.

The three batches of AcsAB whose metal contents were determined contained an average of 1.3 ± 0.3 Ni/$\alpha\beta$ and 17 ± 4 Fe/$\alpha\beta$ (Table 1). To address the possibility that the measured Ni arose from ions that leached from the Ni-NTA column and bound onto the His-tag of AcsAB during purification, the Ni content of the batch purified without this column was also determined. That sample (75% pure) contained 1.7 Ni/$\alpha\beta$ (assuming no Ni in the contaminating proteins), indicating that the Ni ions measured in the Ni-NTA purified samples were associated with AcsAB. A control sample of ACS_{Ct} contained 1.8 Ni/$\alpha\beta$ and 12 Fe/$\alpha\beta$. ACS_{Ct} has been reported to contain 2.0 ± 0.2 Ni/$\alpha\beta$ (n = 10) and 12 ± 2 Fe/$\alpha\beta$ (n = 11).[¶] Thus, our metal analyses suggest that AcsAB contains a full complement of FeS clusters, relative to ACS_{Ct} (i.e., ≥12 Fe/$\alpha\beta$) and 1.0–1.6 Ni/$\alpha\beta$.

The electronic absorption spectrum of thionin-oxidized AcsAB (Fig. 2) revealed a broad absorption shoulder in the 400-nm region, caused by the presence of $[Fe_4S_4]^{2+}$ clusters. Spectral intensity at 420 nm declined when the protein was exposed to CO, reflecting the reduction of these clusters to the 1+ core oxidation state. These spectra were similar to those of ACS_{Ct} (51). The extinction coefficient difference ($\Delta\varepsilon_{420} = \varepsilon_{420}$ oxidized − ε_{420} reduced) quantified to 14.1 mM^{-1}cm^{-1} for AcsAB compared to 14.7 mM^{-1}cm^{-1} for ACS_{Ct} (51). These results suggest that AcsAB and ACS_{Ct} contain the same number and types of FeS clusters.

EPR spectra of three batches of reductant-free partially oxidized AcsAB consisted of two signals (Fig. 3*A*), one with g_{av} = 1.82 (g = 2.01, 1.80, 1.64) and the other with g_{av} = 1.94 (g = 2.04, 1.94, 1.90). At 20 mW and 10 K, the g_{av} = 1.94 and 1.82 signals showed little evidence of saturation (Fig. 3*B*). At temperatures higher than ≈16 K, the g_{av} = 1.82 signal relaxation broadened, whereas the g_{av} = 1.94 signal did not. Quantification of the g_{av} = 1.82 signals yielded an average of 0.28 spin/$\alpha\beta$. In

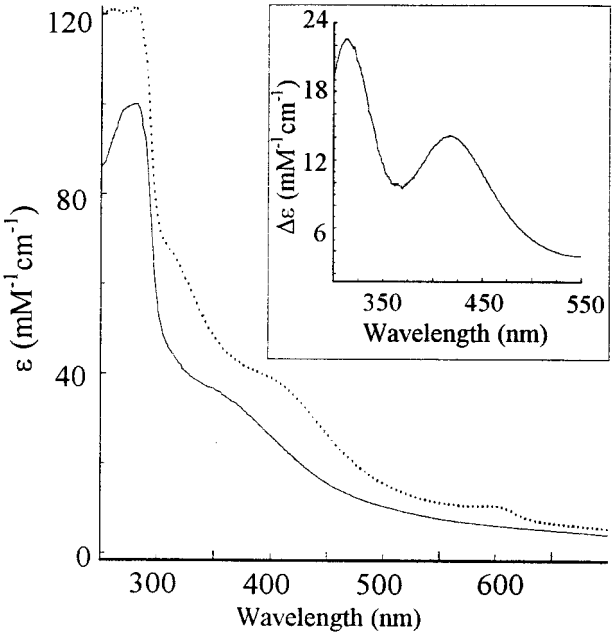

Fig. 2. Electronic absorption spectra of AcsAB. Solid line, AcsAB exposed to 1 atm CO. Dotted line, AcsAB oxidized with a slight excess of thionin. The slight feature in the 600-nm region is attributable to absorption from oxidized thionin. (*Inset*) Oxidized minus-reduced difference spectrum.

[¶]The range of metal contents, CO oxidation, and CO/acetyl-CoA exchange activities given in the text represent compilations of values reported from our laboratory in refs. 2, 5–7, 10, 12–16, 38, 46–51 (indicated uncertainties represent standard deviations).

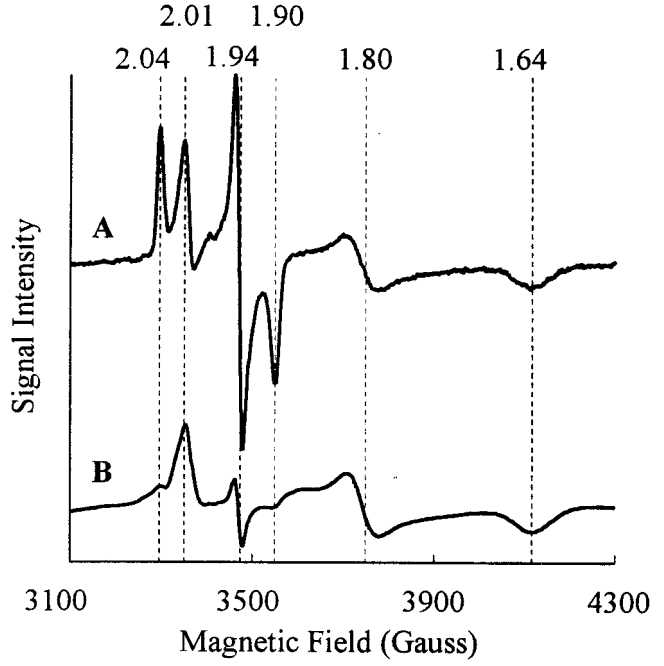

Fig. 3. 10 K X-band EPR spectra of AcsAB (batch 2, 6.8 mg/ml). (*A*) Partially oxidized with thionin, 0.05 mW microwave power; (*B*) same as *A*, but at 20 mW microwave power. Other spectrometer conditions: microwave frequency, 9.42 GHz; modulation frequency, 100 kHz; modulation amplitude, 11.8 G; sweep time, 164 s; time constant, 328 s.

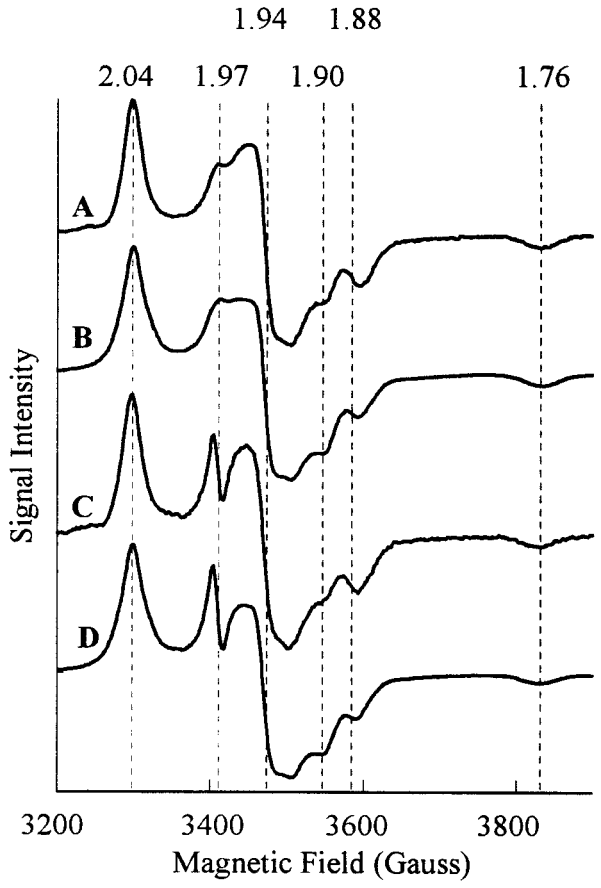

Fig. 4. 10 K X-band EPR spectra of AcsAB. (*A*) CO-reduced (batch 2, 6.8 mg/ml), 0.05 mW microwave power; (*B*) Same as *A*, except 20 mW microwave power; (*C*) CO-reduced (batch 3, 4.6 mg/ml), 0.05 mW microwave power; (*D*) same as *C*, except 20 mW microwave power. Other conditions were as in Fig. 3.

the same redox state, ACS_{Ct} exhibits two signals, a $g_{av} = 1.94$ signal arising from B_{red} and a $g_{av} = 1.82$ signal from C_{red1}. Because the signals in AcsAB have indistinguishable g values and saturation/relaxation properties as those in ACS_{Ct}, we conclude that they arise from clusters with the same structures as the B and C clusters of ACS_{Ct} and refer to them by the same names. Moreover, the average quantified spin intensity of the C_{red1} state of the C cluster in AcsAB (Table 1) is similar to that observed in ACS_{Ct}, indicating a similar proportion of functional C clusters in ACS_{Ct} and AcsAB.

In batches 1 and 2, CO-reduced AcsAB exhibited two EPR signals, one with $g_{av} = 1.94$ and the other with $g_{av} = 1.86$ (g = 1.97, 1.87, 1.75) (Fig. 4*A* and *B*). Essentially indistinguishable signals are observed in spectra of CO-reduced ACS_{Ct}. These signals in ACS_{Ct} arise from B_{red} and C_{red2}, and we conclude that the corresponding signals in AcsAB arise from analogous states. The B_{red} and C_{red2} signals of batch 3 differ slightly from those of batches 1 and 2 (Fig. 4 *C* and *D*). The reason for this is unknown, but the differences probably reflect minor perturbations in protein or cluster structure. The $g_{av} = 1.86$ and $g_{av} = 1.94$ signals from the three batches quantified to an average of 0.14 spin/$\alpha\beta$ and 0.97 spin/$\alpha\beta$, respectively (Table 1). The $g_{av} = 1.94$ signal is $\approx$30% more intense than in ACS_{Ct}, possibly suggesting a shift in spin state from $S = 3/2$ to $S = 1/2$ for the B_{red} state in AcsAB. The intensity of the C_{red2} signal from AcsAB is about half of that reported for ACS_{Ct} (in ACS_{Ct}, both $g_{av} = 1.82$ and 1.86 signals typically quantify to $\approx$0.3 spin/$\alpha\beta$). We may have underestimated the $g_{av} = 1.86$ signal intensity in these spectra, as the dominating $g_{av} = 1.94$ signal is superimposed. Alternatively, the redox potential for the C_{int}/C_{red2} couple may be slightly more negative in AcsAB than in ACS_{Ct}, resulting in a greater proportion of C clusters in the EPR-silent C_{int} state in AcsAB (52). In any event, the presence of the $g_{av} = 1.86$ signal provides conclusive evidence that the C cluster is present in AcsAB and has the same basic structure and properties as that in ACS_{Ct}.

CO-reduced AcsAB did not exhibit the characteristic NiFeC EPR signal of CO-reduced ACS_{Ct}. To address the possibility that AcsAB contained a partially assembled A cluster (an assembled Fe_4S_4 cluster without Ni), the protein was incubated overnight in $NiCl_2$. Ni-treated AcsAB, to be called ACS_{Ec}, exhibited an EPR signal (Fig. 5*B*) with g values, saturation/relaxation properties, and spin intensities (Table 1) indistinguishable from the NiFeC signal of ACS_{Ct}. Thus, we conclude that ACS_{Ec} contains an A cluster with redox and spectroscopic properties similar to that in ACS_{Ct}.

Purified ACS_{Ec} (which exhibited the NiFeC signal when reduced with CO) was loaded on the Ni-NTA agarose column, eluted with 100 mM imidazole, and then subjected to Sephadex G-25 chromatography to remove excess imidazole and Ni. The resulting material did not exhibit the NiFeC signal, suggesting that the Ni-NTA purification step can strip Ni from activated A cluster.

The catalytic properties of ACS_{Ec} and AcsAB were examined. The three batches of AcsAB and ACS_{Ec} exhibited 100 to 250 units/mg of CO oxidation activity (Table 1). The activity of batch 2 is within the range of values observed in our laboratory for fully active ACS_{Ct} (280 $\pm$ 70 units/mg; $n = 44$)[¶]. The higher activity of batch 2 AcsAB and ACS_{Ec} is also consistent with the more intense C cluster signals observed for this batch. Enzyme allowed to incubate overnight in the absence of any reducing agents resulted in a lower intensity of the B_{red} signal and CO oxidation activity, suggesting that AcsAB may not be quite as

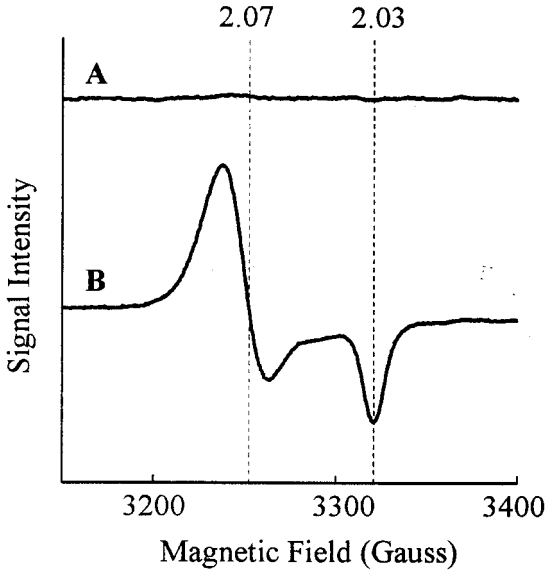

Fig. 5. 130 K X-band EPR spectra of CO-reduced ACS_{Ec} (batch 2, 5.7 mg/ml). (*A*) before addition of $NiCl_2$ and (*B*) after addition of $NiCl_2$. Other spectrometer conditions were as in Fig. 3 except that microwave power was 80 mW.

stable as ACS_{Ct}. None of the AcsAB batches exhibited CO/acetyl-CoA exchange activity, whereas all Ni-treated ACS_{Ec} samples did (Table 1). The activities of batches 2 and 3 were within the range observed for fully functional ACS_{Ct} (0.17 ± 0.10 units/mg; $n = 39$). This result demonstrates that ACS_{Ec} can contain fully assembled and functional A cluster.

Discussion

Our results demonstrate that the *acsAB* genes from *C. thermoaceticum* can be cloned and heterologously expressed in *E. coli* to yield a recombinant protein able to catalyze the oxidation of CO. AcsAB has an $\alpha_2\beta_2$ tetrameric quaternary structure, fully assembled B and C clusters, and at least the Fe_4S_4 component of the A cluster. Because the purification method used seems able to remove the labile Ni from the A cluster, it is unclear whether AcsAB in *E. coli* has a fully assembled A cluster. In any event, an Ni ion can be inserted *in vitro*, affording a fully functional A cluster and enzyme capable of catalyzing CO/acetyl-CoA exchange. The measured redox and spectroscopic properties of these clusters are nearly indistinguishable from those of native ACS_{Ct}. In brief, our results indicate that Ni-treated recombinant enzyme (ACS_{Ec}) is essentially equivalent to native ACS_{Ct}, exhibiting both catalytic activities and the full complement of metal clusters that define this enzyme.

These results and conclusion contrast sharply with those of Roberts *et al.*, who reported that expression of *acsAB* in *E. coli* afforded nonfunctional α and β subunits that migrated independently (17). We obtain functional recombinant enzyme, but of lesser yields, regardless of the strain of *E. coli* used, the growth conditions (anaerobic or bubbled with air,[‖] 15–45°C), or the presence of supplemented Ni in the media. Furthermore, recombinant protein seems relatively stable in its tetrameric form.

The results of this study provide a convenient means for biosynthesizing site-directed mutants of this enzyme. These mutants could be used to identify ligands to the metal centers as well as reveal their role in establishing the catalytic, redox, and/or spectroscopic properties that distinguish these centers. This achievement also provides a means to study metal cluster assembly.

Proteins containing novel metal centers, such as urease, NiFe-hydrogenase, and nitrogenase, have been shown to require *specific* accessory proteins for assembly and insertion of their metal centers (53–58). The previous report of nonfunctional ACS (17) suggested that such proteins were required for the biosynthesis of this metalloenzyme but were absent in *E. coli*. This was easily rationalized, as *E. coli* does not naturally contain ACS, and the metal centers in this enzyme appear to be unique in biology. Therefore, our success was surprising, as it suggests that *E. coli* contains accessory proteins that assemble and insert the B and C clusters into recombinant AcsAB, as well as the FeS component of the A cluster. The B cluster and the Fe_4S_4 components of the C and A clusters may have been assembled and inserted using IscS and IscU, enzymes in *E. coli* that catalyze the formation of FeS clusters (59).

It is intriguing to consider how Ni was inserted into the C cluster *in vivo*. A series of gene clusters in *E. coli* is responsible for assembling the active sites of the organism's three NiFe hydrogenases, including *hya*, *hyb*, *hyc*, and *hyp* (55, 56, 60–63). When *hypB* is deleted, all three hydrogenases lack Ni in their active sites, suggesting that HypB participates in inserting Ni into these sites (36, 37). HypB is a homolog of CooC, a protein involved in inserting Ni into the C cluster of $CODH_{Rr}$ (31). We conjecture that in *E. coli*, HypB served as a *surrogate* of CooC to insert Ni into AcsAB, thereby forming the C cluster. Given that our batches of AcsAB had somewhat variable CO oxidation activity and C cluster EPR signal intensities, this surrogate may not be as effective as CooC in assembling the C cluster.

Whether Ni was inserted into the labile Ni site of the A cluster by accessory proteins in *E. coli* remains unknown. *E. coli* may lack an accessory protein capable of serving as a surrogate for the unidentified accessory protein in *C. thermoaceticum* that is used to insert Ni during A cluster assembly. Alternatively, the Ni in an assembled A cluster may have been lost during purification. Fortunately, Ni could be inserted into this site simply by incubating the enzyme overnight in $NiCl_2$.

Finally, these results impact our understanding of the redox and spin-state heterogeneity that plagues this enzyme. The evidence for heterogeneity is extensive (5, 10, 13–16, 46, 50) and will only be summarized here. Approximately 40% of A clusters contain labile Ni ions, function catalytically, and can be reduced to the A_{red}-CO state (exhibiting the NiFeC signal). The remaining 60% contain nonlabile Ni ions, are nonfunctional, and cannot be reduced. This situation is reflected in the low spin intensity of the NiFeC signal. The C cluster is also heterogeneous. Approximately 40% of C clusters in the C_{ox} state can be reduced by one, two, and three electrons, forming C_{red1}, C_{int}, and C_{red2}, respectively. The remaining 60% can be reduced by one electron to the $C_{S=3/2}$ state. Again, the low spin intensities of the $g_{av} = 1.82$ and 1.86 signals reflect this situation. The B cluster appears to exhibit only spin-state heterogeneity, with about 60% of B_{red} having an $S = ½$ ground state (affording the $g_{av} = 1.94$ signal) and the remainder having $S = 3/2$ (affording EPR features between $g = 4$–6). Obvious reasons for this heterogeneity, including errors in determining protein, metal, or spin concentrations or damage incurred during purification, have been considered and discounted (38). Fraser and Lindahl recently suggested that heterogeneity might arise from events occurring during the growth of *C. thermoaceticum* (16). However, the results presented here indicate that the same type of heterogeneity present in ACS_{Ct} plagues recombinant AcsAB (and ACS_{Ec}). Thus, it would seem that the factors causing heterogeneity are *independent* of the

[‖]Because *E. coli* rapidly consumes O_2 during growth, we are uncertain as to the aerobicity of cultures grown while bubbled with air. The fact that functional recombinant enzyme can be biosynthesized under these conditions merely implies that strict anaerobic conditions are not required.

host organism and of the accessory proteins used to assemble the clusters and are *intrinsic* to the enzyme. Such intrinsic heterogeneity could arise if the two $\alpha\beta$ dimers of the $\alpha_2\beta_2$ tetramer were symmetry-inequivalent.

With active recombinant ACS from *C. thermoaceticum* now available, we plan to prepare site-directed mutants to help elucidate details of the catalytic mechanism of this enzyme and the roles of its metal clusters. We also plan to probe the mechanism of cluster assembly and uncover the origin of the heterogeneity.

Advanced Technology Project Grant 010366–020, National Science Foundation Grant MCB 9604562, and National Institutes of Health Grant GM46441 funded this project.

1. Wood, H. G. & Ljungdahl, L. G. (1991) in *Variations in Autotrophic Life*, eds. Shively, J. M. & Barton, L. L. (Academic, London), pp. 201–250.
2. Kumar, M. & Ragsdale, S. W. (1996) *Chem. Rev.* **96,** 2515–2539.
3. Xia, J., Sinclair, J. F., Baldwin, T. O. & Lindahl, P. A. (1996) *Biochemistry* **35,** 1965–1971.
4. Anderson, M. E. & Lindahl, P. A. (1994) *Biochemistry* **33,** 8702–8711.
5. Lindahl, P. A., Ragsdale, S. W. & Münck, E. (1990) *J. Biol. Chem.* **265,** 3880–3888.
6. Anderson, M. E., DeRose, V. J., Hoffman, B. M. & Lindahl, P. A. (1993) *J. Am. Chem. Soc.* **115,** 12204–12205.
7. Anderson, M. E. & Lindahl, P. A. (1996) *Biochemistry* **35,** 8371–8380.
8. Kumar, M., Lu, W.-P., Liu, L. & Ragsdale, S. W. (1993) *J. Am. Chem. Soc.* **115,** 11646–11647.
9. Seravalli, J., Kumar, M., Lu, W.-P. & Ragsdale, S. W. (1997) *Biochemistry* **36,** 11241–11251.
10. Hu, Z., Spangler, N. J., Anderson, M. E., Xia, J., Ludden, P. W., Lindahl, P. A. & Münck, E. (1996) *J. Am. Chem. Soc.* **118,** 830–845.
11. DeRose, V. J., Anderson, M. E., Lindahl, P. A. & Hoffman, B. M. (1998) *J. Am. Chem. Soc.* **120,** 8767–8776.
12. Xia, J., Dong, J., Wang, S., Scott, R. A. & Lindahl. P. A. (1995) *J. Am. Chem. Soc.* **117,** 7065–7070.
13. Shin, W. & Lindahl, P. A. (1992) *Biochemistry* **31,** 12870–12875.
14. Shin, W. & Lindahl, P. A. (1992) *J. Am. Chem. Soc.* **114,** 9718–9719.
15. Shin, W., Anderson, M. E. & Lindahl, P. A. (1993) *J. Am. Chem. Soc.* **115,** 5522–5526.
16. Fraser, D. M. & Lindahl, P. A. (1999) *Biochemistry* **38,** 15697–15705.
17. Roberts, D. L., James-Hagstrom, J. E., Garvin, D. K., Gorst, C. M., Runquist, J. A., Baur, J. R., Haase, F. C. & Ragsdale, S. W. (1989) *Proc. Natl. Acad. Sci. USA* **86,** 32–36.
18. Ragsdale, S. W., Baur, J. R., Gorst, C. M., Harder, S. R., Lu, W.-P., Roberts, D. L., Runquist, J. A. & Schiau, I. (1990) *FEMS Microbiol. Rev.* **87,** 397–402.
19. Morton, T. A., Runquist, J. A., Ragsdale, S. W., Shanmugasundaram, T., Wood, H. G. & Ljungdahl, L. G. (1991) *J. Biol. Chem.* **266,** 23824–23828.
20. Lu, W. P., Schiau, I., Cunningham, J. R. & Ragsdale, S. W. (1993) *J. Biol. Chem.* **268,** 5605–5614.
21. Ferry, J. G. (1995) *Annu. Rev. Microbiol.* **49,** 305–333.
22. Maupin-Furlow, J. A. & Ferry, J. G. (1996) *J. Bacteriol.* **178,** 340–346.
23. Maupin-Furlow, J. A. & Ferry, J. G. (1996) *J. Bacteriol.* **178,** 6849–6856.
24. Eggen, R. I. L., van Kranenburg, R., Vriesema, A. J. M., Gerrling, A. C. M., Verhagen, M. F. J. M., Hagen, W. R. & de Vos, W. M. (1996) *J. Biol. Chem.* **271,** 14256–14263.
25. Eggen, R. I. L., Gerrling, A. C. M., Jetten, M. S. M. & de Vos, W. M. (1991) *J. Biol. Chem.* **266,** 6883–6887.
26. Bult, C. J., White, O., Olsen, G. J., Zhou, L., Fleischmann, R. D., Sutton, G. G., Blake, J. A., Fitzgerald, L. M., Clayton, R. A., Gocayne, J. D., *et al.* (1996) *Science* **273,** 1058–1073.
27. Klenk, H.-P., Clayton, R. A., Tomb, J.-F., White, O., Nelson, K. E., Ketchum, K. A., Dodson, R. J., Gwinn, M., Hickey, E. K., Peterson, J. D., *et al*. (1997) *Nature* (*London*) **390,** 364–370.
28. Smith, D. R., Doucette-Stamm, L. A., Deloughery, C., Lee, H., Dubois, J., Aldredge, T., Bashirzadeh, R., Blakely, D., Cook, R., Gilbert, K., *et al*. (1997) *J. Bacteriol.* **179,** 7135–7155.
29. Kerby, R. L., Hong, S. S., Ensign, S. A., Coppoc, L. J., Ludden, P. W. & Roberts, G. P. (1992) *J. Bacteriol.* **174,** 5284–5294.
30. Bonam, D. & Ludden, P. W. (1987) *J. Biol. Chem.* **262,** 2980–2987.
31. Kerby, R. L., Ludden, P. W. & Roberts, G. P. (1997) *J. Bacteriol.* **179,** 2259–2266.
32. Spangler, N. J., Meyers, M. R., Gierke, K. L., Kerby, R. L., Roberts, G. P. & Ludden, P. W. (1997) *J. Biol. Chem.* **273,** 4059–4064.
33. Staples, C. R., Heo, J., Spangler, N. J., Kerby, R. L., Roberts, G. P. & Ludden, P. W. (1999) *J. Am. Chem. Soc.* **121,** 11034–11044.
34. Moncrief, M. B. & Hausinger, R. P. (1997) *J. Bacteriol.* **179,** 4081–4086.
35. Soriano, A. & Hausinger, R. P. (1999) *Proc. Natl. Acad. Sci. USA* **96,** 11140–11144.
36. Maier, T., Jacobi, A., Sauter, M. & Böck, A. (1993) *J. Bacteriol.* **175,** 630–635.
37. Maier, T., Lottspeich, F. & Böck, A. (1995) *Eur. J. Biochem.* **230,** 133–138.
38. Shin, W. & Lindahl, P. A. (1993) *Biochim. Biophys. Acta* **1161,** 317–322.
39. Begg, Y. A., Whyte, J. N. & Haddock, B. A. (1977) *FEMS Microbiol. Lett.* **2,** 47–50.
40. Sambrook, J., Fritsch, E. F. & Maniatis, T. (1989) in *Molecular Cloning: A Laboratory Manual*, 2nd Ed., ed. Irwin, N. (Cold Spring Harbor Laboratory Press, Plainview, NY), Chapter 18.
41. Maynard, E. L. & Lindahl, P. A. (1999) *J. Am. Chem. Soc.* **121,** 9221–9222.
42. Xia, J. & Lindahl, P. A. (1995) *Biochemistry* **34,** 6037–6042.
43. Raybuck, S. A., Bastian, N. R., Orme-Johnson, W. H. & Walsh, C. T. (1988) *Biochemistry* **27,** 7698–7702.
44. Orme-Johnson, N. R. & Orme-Johnson, W. H. (1978) *Methods Enzymol.* **52,** 252–257.
45. Pelley, J. W., Garner, C. W. & Little, G. H. (1978) *Anal. Biochem.* **86,** 341–343.
46. Barondeau, D. P. & Lindahl, P. A. (1997) *J. Am. Chem. Soc.* **119,** 3959–3970.
47. Xia, J. & Lindahl, P. A. (1996) *J. Am. Chem. Soc.* **118,** 483–484.
48. Russell, W. K. & Lindahl, P. A. (1998) *Biochemistry* **37,** 10016–10026.
49. Russell, W. K., Stålhandske, C. M. V., Xia, J., Scott, R. A. & Lindahl, P. A. (1998) *J. Am. Chem. Soc.* **120,** 7502–7510.
50. Xia, J., Hu, Z., Popescu, C., Lindahl, P. A. & Münck, E. (1997) *J. Am. Chem. Soc.* **119,** 8301–8312.
51. Shin, W., Stafford, P. R. & Lindahl, P. A. (1992) *Biochemistry* **31,** 6003–6011.
52. Fraser, D. M. & Lindahl, P. A. (1999) *Biochemistry* **38,** 15706–15711.
53. Mulrooney, S. B. & Hausinger, R. P. (1990) *J. Bacteriol.* **172,** 5837–5843.
54. Mobley, H. L. T., Island, M. D. & Hausinger, R. P. (1995) *Microbiol. Rev.* **59,** 451–480.
55. Lutz, S., Jacobi, A., Schlensog, V., Bohm, R., Sawers, G. & Böck, A. (1991) *Mol. Microbiol.* **5,** 123–135.
56. Maier, T. & Böck, A. (1996) in *Mechanisms of Metallocenter Assembly*, ed. Hausinger, R. P. (VCH, New York), pp. 173–192.
57. Dean, D. R., Bolin, J. T. & Zheng, L. (1993) *J. Bacteriol.* **175,** 6737–6744.
58. Allen, R. M., Chatterjee, R., Madden, M. S., Ludden, P. W. & Shah, V. K. (1994) *Crit. Rev. Biotechnol.* **14,** 225–249.
59. Zheng, L., Cash, V. L., Flint, D. H. & Dean, D. R. (1998) *J. Biol. Chem.* **273,** 13264–13272.
60. Menon, N. K., Robbins, J., Peck, H. D., Jr., Chatelus, C. Y., Choi, E.-S. & Przybyla, A. E. (1990) *J. Bacteriol.* **172,** 1969–1977.
61. Menon, N. K., Robbins, J., Wendt, J. C., Shanmugam, K. T. & Przybyla, A. E. (1991) *J. Bacteriol,* **173,** 4851–4861.
62. Menon, N. K., Chatelus, C. Y., DerVartanian, M., Wendt, J. C., Shanmugam, K. T., Peck, H. D., Jr. & Przybyla, A. E. (1994) *J. Bacteriol.* **176,** 4416–4423.
63. Sauter, M., Bohm, R. & Böck, A. (1992) *Mol. Microbiol.* **6,** 1523–1532.